



Antibiotic adsorbability and economic analysis of sodium alginate/chitosan composite-modified semi-carbonized fiber

Jin-ni Wu^{a,†}, Wenkui Mu^{b,†}, Wen-bin Li^{a,*}, Hong-yan Deng^{a,*}, Tianjiang Jin^b,
Touqeer Abbas^c, Yu-ting Song^a, Jia-peng Pan^a, Bixia Wang^a

^aCollege of Environmental Science and Engineering, China West Normal University, Nanchong, Sichuan 637009, China, emails: lw062@163.com (W.-b. Li), dhongyan119@163.com (H.-y. Deng), 1064241904@qq.com (J.-n. Wu), 3268336133@qq.com (Y.-t. Song), 2071514606@qq.com (J.-p. Pan), wangbixia@cwnu.edu.cn (B.-x. Wang)

^bSichuan Chuanqian Expressway Co., Ltd., Gulin 646500, China, emails: 182321481@qq.com (W.-k. Mu), 736588544@qq.com (T.-j. Jin)

^cDepartment of Soil, Water, and Climate, University of Minnesota, Twin 637009, USA, email: abbasouqeer@yahoo.com (A. Touqeer)

Received 26 July 2023; Accepted 13 October 2023

ABSTRACT

The antibiotic adsorbability and economic performance of modified semi-carbonized fiber (SF) were investigated by using 100% chitosan (CS) to modify SF (prepared by cotton) for preparing CS-modified SF (CS-SF). Then, different ratios (0%, 10%, 20%, 50%, 100%, and 200%) of sodium alginate (SA) were used to modify 100CS-SF for preparing SA and CS-modified SF (SA/CS-SF). Batch method was used to investigate the adsorption characteristic of chlortetracycline (CTC), tetracycline (TC), and oxytetracycline (OTC) on different SA/CS-SFs. The effects of temperature, pH, and ionic strength on antibiotic adsorption were compared, and the economic performance of different SA/CS-SFs was analyzed. Results showed that (1) the Langmuir model is suitable for describing the adsorption process of antibiotics by different SA/CS-SFs. The maximum adsorption amount (q_m) of different SA/CS-SFs for CTC, TC, and OTC were 11.17–36.36, 6.14–26.11, and 9.90–32.87 mmol/kg, respectively, ranking in the order of CTC > OTC > TC. (2) The adsorption antibiotics by different SA/CS-SFs conformed to the pseudo-first-order kinetics equation. Antibiotic adsorption on different SA/CS-SFs increased with the increase in temperature, and the adsorption was a spontaneous, endothermic, and entropy-increasing process. (3) In the pH range of 3–9 and ionic strength range of 0.01–0.2 mol/L, the adsorption amount of antibiotics on different SA/CS-SFs all increased first and then decreased with increasing pH and ionic strength, reaching the maximum value at pH = 5 and ionic strength of 0.1 mol/L, respectively. (4) The economy (q_m/price) of different SA/CS-SFs for antibiotic adsorption ranged from 7.18 to 22.91 mg/¥, and 100SA/CS-SF showed the highest economy. Compared with biochar and modified biochar, 100SA/CS-SF had higher economy in antibiotic adsorption.

Keywords: Semi-carbonized fiber; Sodium alginate; Chitosan; Antibiotics; Adsorption amount; Economy

1. Introduction

Antibiotics are drugs that include natural, semi-synthetic, or synthetic compounds that fight pathogens and

affect the growth and development of other cells [1]. The emergence of antibiotics played a revolutionary role in the treatment of human and animal diseases, with strong antibacterial and bactericidal effects. As people's living

* Corresponding authors.

† These authors have contributed equally to this work and share first authorship.

standards improved, the use of antibiotics increased [2]. The metabolism rate of antibiotics in human and livestock is low, and after entering human and livestock bodies, most (>70%) of them are discharged into the environment in their original form [3]. Now, antibiotics are being widely detected in water, feces, crops, soil, animals, and plant samples, which increases the difficulty of their degradation in the environment [4]. Murata et al. [5] investigated antibiotics in 37 rivers throughout Japan and showed that the median value of 12 target antibiotics in 37 rivers was 7.3 ng/L. Nine antibiotics were detected in most of the sea entrances and estuaries of river runoff in the Pearl River delta and estuary, with an average concentration range of 1.2–127 ng/L [6]. 21 antibiotics were detected in surface water and sediment samples from 23 locations in the Fen River, with concentrations ranging from 113.8 to 1,106.0 ng/L [7]. The exposure of antibiotics in the environment presents an increasing trend year by year and has become one of the hotspots of environmental research [8]. The use of antibiotics is sharply increasing and bringing great harm to the environmental system. Thus, the elimination of antibiotic pollutants represented by tetracycline (TC) antibiotics is an urgent matter [9].

Presently, two methods can be mainly used to treat wastewater containing TC antibiotics: biological and physicochemical methods, which involve removing pollutants from water through processes such as adsorption, precipitation, and redox [10,11]. Coagulation sedimentation is simple and easy to implement, but the removal rate is low [12]. Membrane separation method is low cost and has a high removal rate but is prone to secondary pollution [13]. Photocatalytic oxidation is low cost and environmentally friendly but difficult to use on a large scale [14]. In the field of water purification, the adsorption method is widely used. It has high efficiency and is widely applicable in controlling water pollution. Compared with other technologies and methods, adsorption technology does not produce secondary pollution and has excellent adaptability. Therefore, adsorption is considered a prospective method for removing antibiotics in the future. Common adsorbents include activated carbon, graphene, and clay minerals [15]. Chen et al. [16] found that the adsorption behavior of TC by activated sludge at temperatures of 10°C and 25°C conformed to the Langmuir model, with maximum adsorption of 31.14 and 70.95 mg/g, respectively, and when the temperature increased to 40°C, the adsorption process conformed to the Henry model. Tang et al. [17] adsorbed TC using magnetic metal–organic frameworks produced by the hydrothermal method, and the maximum saturated adsorption amount of 20.89 mg/g was reached under certain conditions. Deng et al. [18] used amphoteric modifier and magnetization to treat biochar materials, which significantly improved the adsorption capacity of biochar for TC.

Fibers are effective adsorbent materials due to their porous structure and large surface area. Studies found that fiber materials have a faster adsorption rate and higher adsorption capacity for heavy metal ions [19]. Kinetic and isotherm studies, whether on single- or multi-metal solutions, show that fiber materials prepared by ion imprinting have a faster adsorption rate and a higher adsorption performance for Pd(II) [20]. Carbonized fiber, when used

for adsorption of pollutants, has the advantages of a large surface area, abundant pore structure and active sites, broad spectrum, sustainability, and degradability. Sewage sludge produced by activated sludge sewage was carbonized, extruded, formed, and sintered at 900°C. The average pore size and pore volume of the carbonized sludge were 3.93 nm and 0.0092 cm³/g, respectively [21]. The structure of semi-carbonized straw fibers shows a large number of micropores, and acidic oxygen-containing groups endow the structure with higher adsorption of polar molecules [22].

From the economic point of view, biological materials that undergo carbonization and modification to improve their adsorption performance are effective adsorbents. Hussein et al. [23] found that the preparation of activated carbon from agricultural wastes has high adsorption performance on heavy oil and can be recycled six times with great economic benefits. If the carbonized fibers are modified again, then the adsorption of pollutants by the fiber materials can be greatly improved, and its economy is relatively improved at the same time. Few related studies and reports have been published on this topic. In this research, cotton was used as the raw material for the production of semi-carbonized fiber (SF), and then chitosan (CS) and sodium alginate (SA) were used for composite modification of SF to explore the effects of different modification ratios. The adsorption characteristics and adsorption kinetics of TC antibiotics, as well as the effects of pH, temperature, and ionic strength on the adsorption process were studied. In addition, an economic analysis of the composite-modified SF was conducted. This research aims to provide a theoretical basis for the development of composite-modified materials for the adsorption of antibiotic contaminants.

2. Materials and methods

2.1. Experimental materials

2.1.1. Experimental modifier and pollutants

CS (Shanghai YuanYe Biotechnology Co., Ltd., China, analytic reagent) with 90% purity was used as single modifier. SA (Chengdu Cologne Chemical Co., Ltd., China, analytic reagent) was used as the composite modifier. Chlortetracycline (CTC), TC, and oxytetracycline (OTC) with purities exceeding 99% were sourced from Shanghai Aladdin Biochemical Technology Co., Ltd., China. The molecular formula of the two modifiers is shown in Fig. 1a and b.

2.1.2. Preparation of composite-modified SF

Raw cotton was placed in a muffle furnace at 300°C and stored in an anaerobic environment for 2 h. After being cooled, the material was ground through a 60-mesh screen to obtain SF. A certain mass of SF was weighed and added to the pre-prepared CS solution at a solid–liquid ratio of 10:1. The reaction was maintained at a constant temperature of 60°C for 4 h in a water bath with constant stirring. The material was then centrifuged at 4,800 rpm for 10 min, and the supernatant was discarded to obtain CS-modified SF (CS-SF), which was washed three times by centrifugal separation. After being dried at 60°C, it was ground through a 60-mesh nylon sieve and sealed for later use. CS-SF was

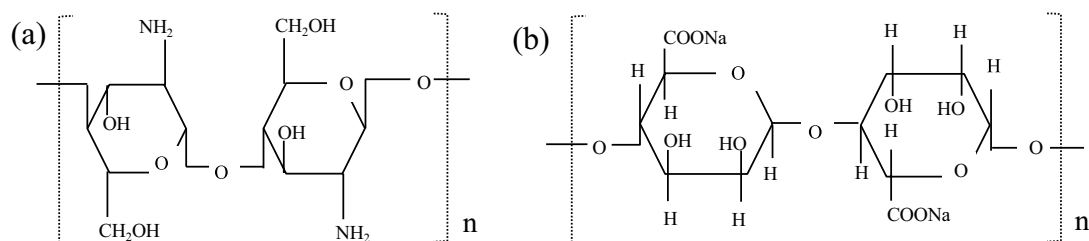


Fig. 1. Molecular formula of chitosan (a) and sodium alginate (b).

composite-modified with SA by the same method. The samples were dried, ground, and screened to obtain SA-modified CS-SF (SA/CS-SF). The five types of SA/CS-SF that were obtained were 10SA/CS-SF (10% SA-modified CS-SF, the same as the rest of the materials), 20SA/CS-SF, 50SA/CS-SF, 100SA/CS-SF, and 200SA/CS-SF. The dosages of SA and CS were calculated according to the wet method [24].

2.2. Experimental design

2.2.1. Isothermal adsorption experiment

The concentrations of CTC, TC, and OTC were set at nine concentration gradients of 0.3, 0.6, 1.2, 3, 6, 12, 18, 24, and 30 mg/L [24]. The temperature was set at 20°C, the pH value of the solution was set as 7, and the ionic strength was set as 0.1 mol/L NaCl.

2.2.2. Kinetics adsorption of antibiotics

The adsorption time was set as 5, 10, 15, 30, 60, 120, 180, 240, 300, 360, 480, 600, and 720 min. The temperature was set as 20°C, the pH value of the solution was set as 7, and the ionic strength was set as 0.1 mol/L NaCl.

2.2.3. Influence of experimental factors

The experimental temperatures were set at 10°C, 20°C, and 30°C; the pH of the solution was set at 7; and the ionic strength was set at 0.1 mol/L NaCl. The initial pH values of the solution were set as 3, 5, 7, and 9; the solution temperature was set as 20°C; and the ionic strength was set as 0.1 mol/L NaCl. The initial ionic strength of the solution was set to 0.01, 0.1, and 0.2 mol/L NaCl; the solution temperature was set to 20°C; and the pH value was set to 7.

2.3. Experimental methods

2.3.1. Isothermal and kinetics adsorption

Batch equilibrium method was used for antibiotic adsorption. A total of 0.2000 g of the sample was weighed in 50 mL plastic centrifuge tubes and added with 20 mL of antibiotic solutions with different concentration gradients. The samples were oscillated at 25°C and 200 rpm for 12 h at constant temperature [25] and centrifuged at 4,800 rpm for 10 min. The concentration of antibiotics in the supernatant was determined by high-performance liquid chromatography, and the equilibrium adsorption amount was calculated by subtraction method. All the above measurements

were inserted into standard solution for analytical quality control.

2.3.2. Economic analysis

The q_m and price of different materials were used to calculate the economic performance. The economy (mg/¥) was defined as the ratio of q_m (mmol/kg) to price (¥/g). The price of all materials and modifiers were calculated using the average of the market price.

2.4. Data processing

2.4.1. Calculation of equilibrium adsorption capacity

The equilibrium adsorption capacity can be calculated according to Eq. (1):

$$q = \frac{(c_0 - c_e)V}{m} \quad (1)$$

where V is the volume of solution (mL); c_0 is the antibiotic concentration at the starting point (mmol/L); c_e is the antibiotic concentration at the equilibrium point (mmol/L); m is the mass of tested sample (g); and q is the equilibrium adsorption capacity of tested sample for antibiotics (mmol/kg).

2.4.2. Fitting of adsorption isotherms

The Langmuir model [26] was selected to fit the adsorption isotherms of the three antibiotics according to the adsorption isotherm trend [Eq. (2)]:

$$q = \frac{q_m b c_e}{1 + b c_e} \quad (2)$$

where q_m is the maximum adsorption amount of antibiotics for the tested sample, mmol/kg; b is the apparent equilibrium constant of antibiotic adsorption on the tested sample for the measurement of adsorption affinity.

2.4.3. Fitting of adsorption kinetics model

The pseudo-first-order and pseudo-second-order kinetics equation models were used to simulate the adsorption process of three antibiotics on different modified materials [27]. The kinetics equations are defined as Eqs. (3) and (4):

$$\ln(q - q_t) = \ln q - k_1 t \quad (3)$$

$$\frac{t}{q_t} = \frac{1}{q^2 k_2} + \frac{t}{q} \tag{4}$$

where q_t is the adsorption capacity corresponding to the adsorbent at time t (mmol/kg); k_1 and k_2 are pseudo-first-order and pseudo-second-order reaction rate constants, respectively; t is the adsorption time (min).

CurveExpert 1.4 fitting software was used in isothermal fitting, and Origin 9.0 was adopted to improve data plotting. SPSS 16.0 statistical analysis software was used to process the experimental data for variance and correlation analysis.

3. Results and discussion

3.1. Isothermal adsorption of antibiotics on different SA/CS-SFs

The adsorption isotherms of CTC, TC, and OTC on each test SA/CS-SF under the conditions of 20°C, pH = 7, and ionic strength of 0.1 mol/L are shown in Fig. 2a–c. The antibiotic adsorption capacity of different SA/CS-SFs increased with the increase in equilibrium concentration, presenting L-shaped adsorption curves. The Langmuir model was used to fit the adsorption isotherms of CTC, TC, and OTC by the SA/CS-SFs (Table 1), and the fitting correlation reached a highly significant level ($P < 0.01$), which indicated that the adsorption of antibiotics on the SA/CS-SFs conformed to the Langmuir model. The maximum adsorption capacity (q_m) values of CTC, TC, and OTC on each SA/CS-SF were 11.17–36.36, 6.14–26.11, and 9.90–32.87 mmol/kg, respectively, ranking in the order of CTC > OTC > TC, consistent with the results shown by the adsorption isotherm in Fig. 2. Compared with those of raw SF, the q_m values of antibiotics on CS-SF increased by 23.45%–25.66%, and the q_m values of antibiotics on different SA/CS-SFs increased by 30.80%–325.24%. Moreover, 100SA/CS-SF had the highest adsorption capacity for antibiotics among all treatments under the same condition. The adsorption constant (b) in the Langmuir model for antibiotic adsorption changed from 19.37–144.49, indicating that SA/CS-SF had strong affinity for antibiotics. The modification of materials enriched the functional group of SF, thus promoting the reaction between antibiotics and SF materials and facilitating the adsorption of antibiotics [28]. The above results are similar to those of modification of clay, biochar, and other materials [29].

3.2. Adsorption kinetic characteristics of antibiotics

The adsorption kinetic curves of CTC, TC, and OTC on the tested SA/CS-SFs are illustrated in Fig. 3a–c. CTC, TC, and OTC all reached adsorption equilibrium at approximately 240 min. The adsorption process of antibiotics on the SA/CS-SFs was simulated using pseudo-first-order and pseudo-second-order kinetic equation models (Table 2). The adsorption kinetics of all antibiotics conformed to the pseudo-first-order kinetic equation. The R^2 values of the pseudo-first-order kinetic equation for antibiotic adsorption were higher than those of the pseudo-second-order kinetic equation. Therefore, the pseudo-first-order kinetic equation

Table 1
Fitting parameters of the antibiotic adsorption isotherms

	Treatment	q_m	b	S	r
Chlortetracycline	SF	11.17	28.03	8.32	0.9815**
	CS-SF	13.87	27.02	9.91	0.9826**
	10SA/CS-SF	14.61	29.77	2.99	0.9984**
	20SA/CS-SF	19.21	53.06	5.73	0.9978**
	50SA/CS-SF	17.35	45.48	8.55	0.9938**
	100SA/CS-SF	36.36	38.43	22.34	0.9849**
	200SA/CS-SF	28.68	20.17	2.46	0.9990**
Tetracycline	SF	6.14	121.75	28.95	0.9797**
	CS-SF	7.58	98.80	18.56	0.9880**
	10SA/CS-SF	12.84	99.62	9.95	0.9967**
	20SA/CS-SF	17.58	35.67	3.51	0.9984**
	50SA/CS-SF	16.03	25.38	2.29	0.9989**
	100SA/CS-SF	26.11	19.37	3.53	0.9973**
	200SA/CS-SF	19.90	38.46	4.74	0.9980**
Oxytetracycline	SF	9.90	144.49	32.83	0.9743**
	CS-SF	12.44	25.63	2.44	0.9985**
	10SA/CS-SF	13.28	42.83	3.25	0.9987**
	20SA/CS-SF	18.02	41.58	7.65	0.9943**
	50SA/CS-SF	16.56	24.99	3.57	0.9971**
	100SA/CS-SF	32.87	26.06	8.9	0.9933**
	200SA/CS-SF	26.11	19.37	3.53	0.9973**

Note: ** indicates significant correlation at the $P = 0.01$ level.

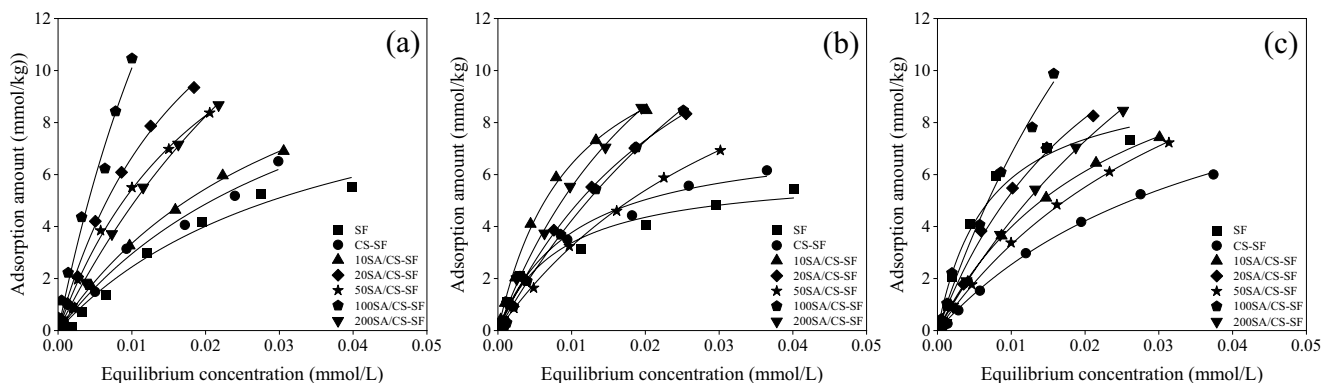


Fig. 2. Adsorption isotherms of chlortetracycline (a), tetracycline (b), and oxytetracycline (c) on different SA/CS-SFs.

model accurately described the adsorption of CTC, TC, and OTC on different SA/CS-SFs. The above results indicated that the adsorption of CTC, TC, and OTC by each tested SA/CS-SF was mainly affected by the transfer resistance of antibiotic molecules [30].

3.3. Effect of temperature on antibiotics adsorption

The antibiotic adsorption capacity of different SA/CS-SFs increased with the increase in temperature in the range of

10°C–30°C, showing a positive temperature effect (Fig. 4a–c). The adsorption amount of CTC, TC, and OTC increased by 13.11%–48.85%, 12.77%–40.52%, and 20.97%–47.96%, respectively. The promoting effect was observed after SA was modified again, so its warming effect was enhanced. With the increase in temperature, the rate of diffusion of antibiotic molecules in solution increased. Thus, the chance of contact between antibiotics and SA/CS-SF increased. A higher temperature corresponds to a better adsorption effect of the test SA/CS-SF on antibiotics.

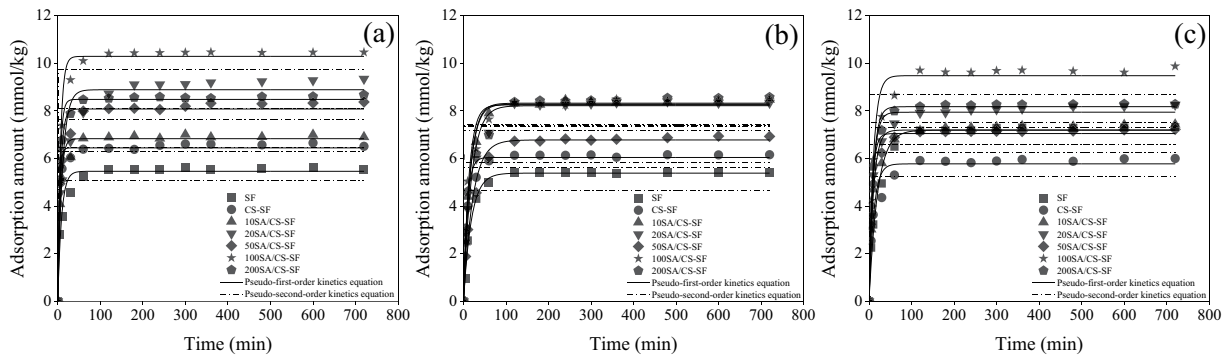


Fig. 3. Adsorption kinetics of chlortetracycline (a), tetracycline (b), and oxytetracycline (c).

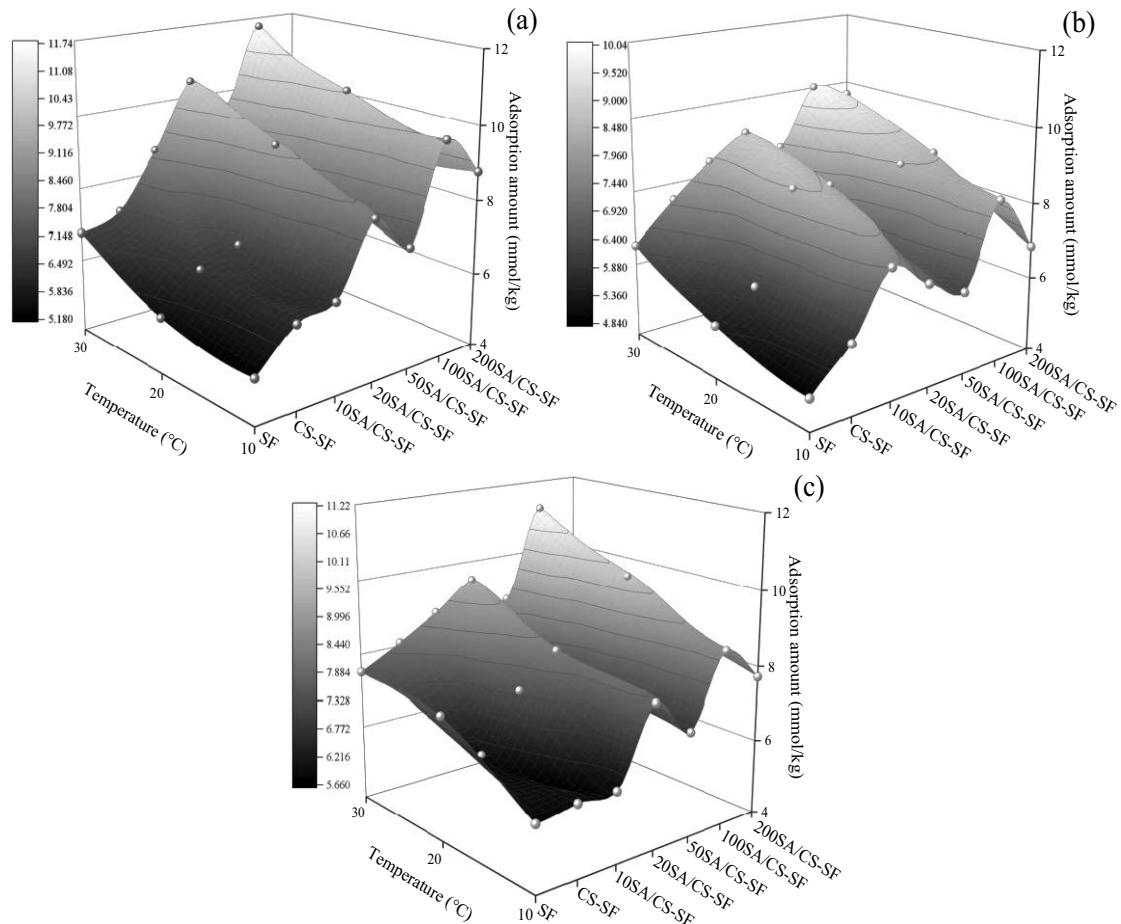


Fig. 4. Effect of temperature on the adsorption of chlortetracycline (a), tetracycline (b), and oxytetracycline (c).

The thermodynamic parameters of CTC, TC, and OTC adsorption by different SA/CS-SFs are shown in Table 3. The Gibb's free energy variation (ΔG) of CTC, TC, and OTC adsorption by different SA/CS-SFs under the conditions of 10°C and 30°C were less than 0, thus indicating that the adsorption process was spontaneous. The spontaneity was stronger at 30°C under the same treatment. The enthalpy change (ΔH) of antibiotic adsorption on the SA/CS-SFs was positive, indicating that the adsorption process was endothermic, and temperature increase was conducive to their adsorption of metal ions, which is consistent with the positive

temperature effect shown in Fig. 3. The entropy changes (ΔS) of antibiotic adsorption in all tested SA/CS-SFs were all greater than zero, indicating that the adsorption process was an entropy-increasing reaction, which was mainly due to the different antibiotic adsorption mechanisms on the SA/CS-SFs, leading to increased system confusion [31].

3.4. Effect of pH and ionic strength on antibiotic adsorption

The adsorption amount of CTC, TC, and OTC on each tested SA/CS-SF increased first and then decreased with

Table 2
Fitting parameters of chlortetracycline, tetracycline, and oxytetracycline adsorption kinetics

Treatments	Pseudo-first-order kinetic equation		Pseudo-second-order kinetic equation		
	q_e (mmol/kg)	R^2	q_e (mmol/kg)	R^2	
Chlortetracycline	SF	6.45	0.9699**	6.07	0.7579**
	CS-SF	6.47	0.9815**	6.30	0.9254**
	10SA/CS-SF	7.05	0.9710**	6.63	0.7577**
	20SA/CS-SF	7.73	0.9626**	7.23	0.7319**
	50SA/CS-SF	7.57	0.9734**	7.23	0.8234**
	100SA/CS-SF	8.36	0.9881**	8.12	0.9163**
	200SA/CS-SF	8.31	0.9853**	7.97	0.8604**
Tetracycline	SF	2.11	0.9760**	1.94	0.6093**
	CS-SF	2.45	0.9741**	2.32	0.7899**
	10SA/CS-SF	3.27	0.9935**	3.04	0.6875**
	20SA/CS-SF	4.14	0.9752**	3.87	0.7214**
	50SA/CS-SF	3.97	0.9875**	3.71	0.7061**
	100SA/CS-SF	4.84	0.9920**	4.49	0.6851**
	200SA/CS-SF	4.23	0.9505**	3.85	0.6037**
Oxytetracycline	SF	4.75	0.9696**	4.39	0.6655**
	CS-SF	5.13	0.9628**	4.82	0.7384**
	10SA/CS-SF	6.86	0.9430**	6.43	0.7248**
	20SA/CS-SF	7.31	0.9494**	6.92	0.7693**
	50SA/CS-SF	7.26	0.9556**	6.82	0.7477**
	100SA/CS-SF	9.03	0.9376**	8.64	0.8134**
	200SA/CS-SF	8.30	0.9463**	8.03	0.8672**

Note: ** indicates significant correlation at the $P = 0.01$ level.

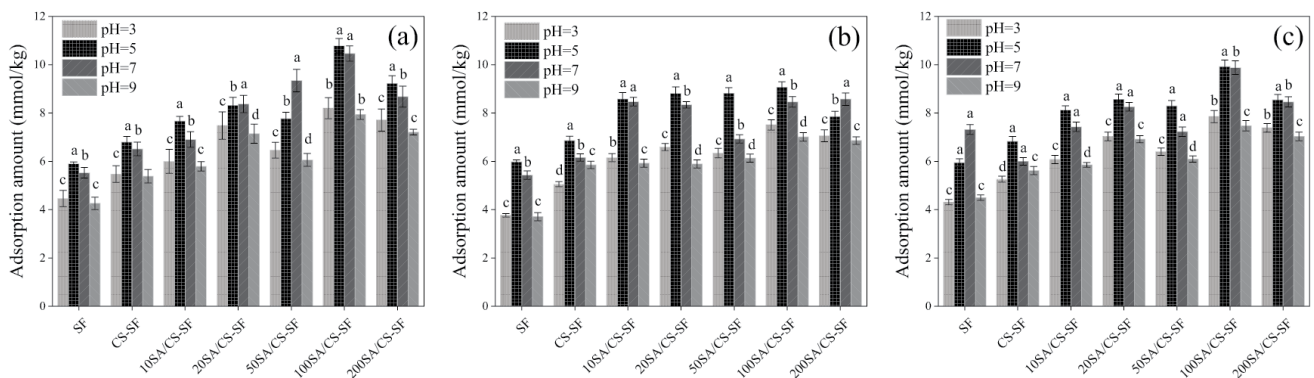


Fig. 5. Effect of pH on the adsorption of chlortetracycline (a), tetracycline (b), and oxytetracycline (c). Note: different lowercase letters indicate significant differences between treatments at $P = 0.05$ level.

Table 3
Thermodynamic parameters of chlortetracycline, tetracycline, and oxytetracycline adsorption

Treatment	ΔG (kJ/mol)		ΔH (kJ/mol)	ΔS (J/mol-K)	
	10°C	30°C			
Chlortetracycline	SF	-27.83	-29.94	2.69	107.81
	CS-SF	-27.68	-29.74	2.65	107.12
	10SA/CS-SF	-26.94	-29.01	2.72	104.7
	20SA/CS-SF	-24.75	-26.80	2.94	97.79
	50SA/CS-SF	-24.91	-27.03	3.01	98.60
	100SA/CS-SF	-23.52	-25.34	2.75	92.77
	200SA/CS-SF	-24.88	-26.61	2.48	96.61
	Tetracycline	SF	-24.11	-25.81	2.52
CS-SF		-23.90	-25.58	2.52	93.28
10SA/CS-SF		-25.11	-26.88	2.52	97.56
20SA/CS-SF		-24.68	-26.42	2.52	96.03
50SA/CS-SF		-23.84	-25.52	2.52	93.07
100SA/CS-SF		-25.55	-27.35	2.52	99.11
200SA/CS-SF		-23.24	-24.88	2.52	90.96
Oxytetracycline		SF	-26.20	-28.65	3.29
	CS-SF	-23.51	-25.20	2.56	92.06
	10SA/CS-SF	-23.71	-25.96	3.35	95.56
	20SA/CS-SF	-25.49	-27.42	2.70	99.55
	50SA/CS-SF	-23.73	-25.56	2.74	93.48
	100SA/CS-SF	-24.96	-27.06	2.98	98.67
	200SA/CS-SF	-23.12	-24.98	2.86	91.74

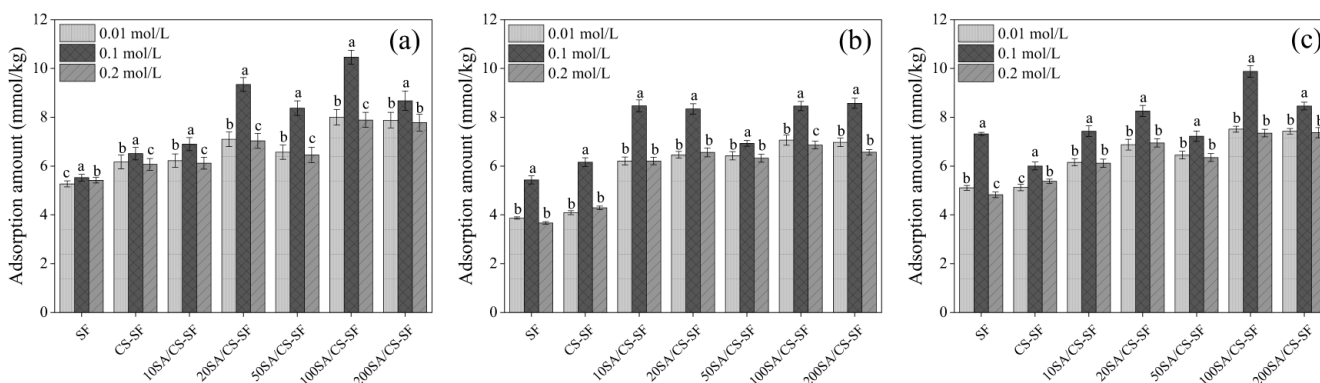


Fig. 6. Effect of ionic strength on the adsorption of chlortetracycline (a), tetracycline (b), and oxytetracycline (c).

the increase in pH when the pH value was in the range of 3–9 (Fig. 5a–c), reaching the maximum at pH = 5. When the pH increased from 3 to 5, the adsorption amount of the antibiotics on the SA/CS-SFs increased by 11.23%–58.62%, whereas the adsorption amount decreased by 14.18%–37.96% when the pH increased from 5 to 9. The pH of the solution had a great influence on the antibiotic adsorption, which may be related to the existence of antibiotics in the aqueous solution. Antibiotics with pH < 3.30 are positively charged, those with pH between 3.30 and 7.69 are positively and negatively charged, and those with pH > 9.50 exist as an anion. Therefore, under pH = 5, antibiotics can be combined with SA/CS-SF by cation exchange and

hydrophobic bond. With increasing pH, the proportion of negative charge in the antibiotic molecule increased and the adsorption decreased gradually [32].

Fig. 6a–c shows the effect of ionic strength on the adsorption of TC, OTC, and CTC by the tested SA/CS-SFs. With increasing ionic strength, the adsorption amount of antibiotics on the tested SA/CS-SFs increased first and then decreased, reaching the maximum at 0.1 mol/L. When the ionic strength increased from 0.01 to 0.1 mol/L, the adsorption amount of the antibiotics on the tested SA/CS-SFs increased by 4.86%–31.63% (TC), 7.91%–50.56% (OTC), and 12.02%–43.29% (CTC). Low Na⁺ concentration in the solution enhanced the solubility of antibiotics. When the ionic

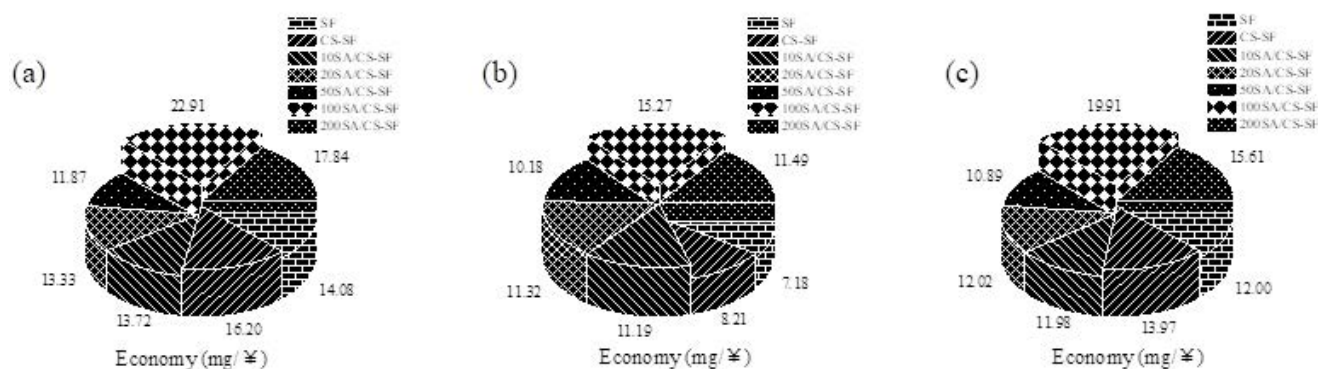


Fig. 7. Economy of chlortetracycline (a), tetracycline (b), and oxytetracycline (c) adsorption by the SA/CS-SFs.

strength increased from 0.1 to 0.2 mol/L, the concentration of Na^+ in the solution was high, the antibiotic molecules were not easily released, and the solubility of the antibiotics decreased [33].

3.5. Economic analysis of the different SA/CS-SFs

The economy (q_m/price) of each tested SA/CS-SF for CTC, TC, and OTC adsorption is illustrated in Fig. 7a–c. The economy of different SA/CS-SFs ranged from 13.33–22.91 (CTC), 7.18–15.27 (TC), and 10.89–19.91 (OTC) mg/¥, with 100SA/CS-SF showing the highest economy. The economy of the tested SA/CS-SF showed that 100SA/CS-SF > 200SA/CS-SF > SA/CS-SF > 10SA/CS-SF > 20SA/CS-SF > 50SA/CS-SF > SF. This result was due to the fact that a higher proportion of SA modification corresponds to a larger amount of SA drug used. Thus, the cost increased. CTC, TC, and OTC adsorbed by 100SA/CS-SF had the highest economy among all the tested materials, increasing by 72.91–123.58% compared with that of SF. The q_m of TC by biochar was 19.90 mmol/kg, and the economy of biochar for TC adsorption was 13.61 mg/¥ [26]. The q_m of TC by amphoteric-magnetized carbon-based clay and amphoteric-magnetized biochar was 14.30 and 13.69 mmol/kg, respectively [18], and their economy was 12.46 and 12.94 mg/¥, respectively. Compared with biochar and modified biochar, 100SA/CS-SF had higher economy in antibiotic adsorption. In addition, the tested SA/CS-SFs have the advantages of sustainability and degradability, which indicated that the antibiotic adsorption by SA/CS-SFs was economically feasible.

4. Conclusion

The q_m of different SA/CS-SFs for antibiotic was 6.14–36.36 mmol/kg, ranking in the order of CTC > OTC > TC. The antibiotic adsorption by different SA/CS-SFs was mainly affected by the transfer resistance of antibiotic molecules. Antibiotic adsorption on different SA/CS-SFs increased with the increase in temperature, showing a spontaneous, endothermic, and entropy-increasing process. The adsorption amount of antibiotics on different SA/CS-SFs all increased first and then decreased with increasing pH and ionic strength, reaching the maximum value at pH = 5 and ionic strength of 0.1 mol/L, respectively. The economy of different SA/CS-SFs for antibiotic adsorption ranged from 7.18

to 22.91 mg/¥, and 100SA/CS-SF showed the highest economy. Compared with biochar and modified biochar, 100SA/CS-SF had higher economy in antibiotic adsorption.

Acknowledgements

The authors wish to acknowledge and thank the Sichuan Transportation Technology Project (2021-ZL-8), the Fundamental Research Funds of China West Normal University (18B023; 20A022), and the Tianfu Scholar Program of Sichuan Province (2020-17).

Conflict of interests

The authors declare that they have no conflict of interest.

References

- [1] H.D. Zhou, L.P. Huang, X.M. Chen, D.Y. Li, J.Y. Cui, Removal of antibiotics and antibiotic resistance genes from urban rivers using artificial ecosystems, *Environ. Sci.*, 42 (2021) 850–859.
- [2] F.K. Zhao, L. Yang, L.D. Chen, S.J. Li, L. Sun, Co-contamination of antibiotics and metals in peri-urban agricultural soils and source identification, *Environ. Sci. Pollut. Res.*, 25 (2018) 34063–34075.
- [3] Y. Zou, H.Y. Deng, M. Li, Y.H. Zhao, W.B. Li, Enhancing tetracycline adsorption by riverbank soils by application of biochar-based composite materials, *Desal. Water Treat.*, 207 (2020) 332–340.
- [4] J.J. Zhang, J. Chen, P.F. Wang, Pollution characteristics of four-type antibiotics in typical lakes in China, *Chin. Environ. Sci.*, 41 (2021) 4271–4283.
- [5] A. Murata, H. Takada, K. Mutoh, H. Hosoda, A. Harada, N. Nakada, Nationwide monitoring of selected antibiotics: distribution and sources of sulfonamides, trimethoprim, and macrolides in Japanese rivers, *Sci. Total Environ.*, 409 (2011) 5305–5312.
- [6] W.H. Xu, W. Yan, X.D. Li, Y.D. Zou, X.X. Chen, W.X. Huang, L. Miao, R.J. Zhang, G. Zhang, S.C. Zou, Antibiotics in riverine runoff of the Pearl River delta and Pearl River estuary, China: concentrations, mass loading and ecological risks, *Environ. Pollut.*, 182 (2013) 402–407.
- [7] L.F. Wang, H. Li, J.H. Dang, H. Guo, Y.E. Zhu, W.H. Han, Occurrence, distribution, and partitioning of antibiotics in surface water and sediment in a typical tributary of Yellow River, China, *Environ. Sci. Pollut. Res.*, 28 (2021) 28207–28221.
- [8] Q.Q. Zhang, G.G. Ying, C.G. Pan, Y.S. Liu, J.L. Zhao, Comprehensive evaluation of antibiotics emission and fate in the river basins of China: source analysis, multimedia modeling,

- and linkage to bacterial resistance, *Environ. Sci. Technol.*, 49 (2015) 6772–6782.
- [9] J.Q. Zhang, Y.J. Chen, F.H. Wang, B. Zhao, Adsorption characteristics of tetracycline hydrochloride onto bentonite, *Chin. J. Environ. Eng.*, 10 (2016) 4808–4814.
- [10] H.Y. Zhan, Q.X. Zhou, Research progress on treatment technology of tetracycline antibiotics pollution in the environment, *J. Environ. Eng. Technol.*, 11 (2021) 571–581.
- [11] W. Liu, H. Wang, X.J. Chen, D.W. Yang, G.W. Kuang, Z.L. Sun, Progress on degradation of antibiotics in environment, *Prog. Vet. Med.*, 30 (2009) 89–94.
- [12] S. Tohru, S. Kenji, F. Kohei, O. Yusuke, Rapid removal of tetracycline antibiotics from water by coagulation–flotation of sodium dodecyl sulfate and poly(allylamine hydrochloride) in the presence of Al(III) ions, *Sep. Purif. Technol.*, 187 (2017) 76–83.
- [13] S.Z. Li, X.Y. Li, D.Z. Wang, Membrane (RO-UF) filtration for antibiotic wastewater treatment and recovery of antibiotics, *Sep. Purif. Technol.*, 187 (2017) 76–83.
- [14] H.X. Wang, B. Liao, T. Lu, Y.L. Ai, G. Liu, Enhanced visible-light photocatalytic degradation of tetracycline by a novel hollow BiOCl@CeO₂ heterostructured microspheres: structural characterization and reaction mechanism, *J. Hazard. Mater.*, 385 (2020) 121552, doi: 10.1016/j.jhazmat.2019.121552.
- [15] O. Yaqubi, M.H. Tai, D. Mitra, C. Gerente, K.G. Neoh, C.H. Wang, Y. Andres, Adsorptive removal of tetracycline and amoxicillin from aqueous solution by leached carbon black waste and chitosan-carbon composite beads, *J. Environ. Chem. Eng.*, 9 (2021) 104988–104988.
- [16] R.P. Chen, L. Zhang, J. Yu, Y. Tao, Z.P. Zhang, K.X. Li, D.F. Liu, Study on the sorption behavior of tetracycline onto activated sludge, *Environ. Sci.*, 33 (2012) 156–162.
- [17] Z.X. Tang, Y. Wang, Y. Sun, G.M. Lu, Preparation of Fe₃O₄@PDA@MIL-101(Cr) and its adsorption to tetracycline, *Liaoning Chem. Ind.*, 47 (2018) 728–732.
- [18] H.Y. Deng, H.X. He, W.B. Li, T. Abbas, Z.F. Liu, Characterization of amphoteric bentonite-loaded magnetic biochar and its adsorption properties for Cu²⁺ and tetracycline, *PeerJ*, 10 (2022) 13030–13049.
- [19] L.H. Zhang, Z. Wu, Study on a new chelating fiber adsorption of Pb(II) and Cd(II), *Adv. Mater. Res.*, 864 (2014) 1394–1398.
- [20] S. Lin, W. Wei, X.H. Wu, T. Zhou, J. Mao, Y.S. Yun, Selective recovery of Pd(II) from extremely acidic solution using ion-imprinted chitosan fiber: adsorption performance and mechanisms, *J. Hazard. Mater.*, 299 (2015) 10–17.
- [21] Y.S. Yoo, J.H. Jo, G.T. Seo, Characteristics of pollutants removal by carbonized porous media made from sewage sludge, *Mater. Sci. Forum*, 804 (2014) 99–102.
- [22] W.B. Li, M.T. Guo, Y.F. Wang, H.Y. Deng, H. Lei, C.T. Yu, Z.F. Liu, Selective adsorption of heavy metal ions by different composite-modified semi-carbonized fibers, *Sep. Purif. Technol.*, 328 (2023) 125022, doi: 10.1016/j.seppur.2023.125022.
- [23] M. Hussein, A.A. Amer, I.I. Sawzan, Oil spill sorption using carbonized pith bagasse. Application of carbonized pith bagasse as loose fiber, *Global Nest J.*, 11 (2009) 440–448.
- [24] Y.F. Wang, W.B. Li, H.Y. Deng, L. Zhu, J.Q. Li, M.T. Guo, Z.F. Liu, Effect mechanism of litter extract from *Alternanthera philoxeroides* on the selective absorption of heavy metal ions by amphoteric purple soil, *J. Environ. Manage.*, 321 (2022) 115970, doi: 10.1016/j.jenvman.2022.115970.
- [25] Y.F. Wang, H.Y. Deng, W.B. Li, A. Touqeer, M. Li, J.N. Wu, J.M. Ouyang, Litter extract from *Alternanthera philoxeroides* as an efficient passivator for oxytetracycline stability in riverbank purple soils, *Environ. Technol. Innovation*, 29 (2023) 103022, doi: 10.1016/j.eti.2023.103022.
- [26] W.B. Li, X.Y. Chen, H.Y. Deng, D. Wang, J.C. Jiang, Y.Z. Zeng, L. Kang, Z.F. Meng, Effects of exogenous biochar on soil tetracycline adsorption in Jialing River Basin, *Chin. J. Soil Sci.*, 51 (2020) 487–495.
- [27] R.A. Figueroa, A.A. Leonard, A.A. Mackay, Modeling tetracycline antibiotic sorption to clays, *Environ. Sci. Technol.*, 38 (2004) 476–483.
- [28] S.J. Zhang, S.X. Chen, Q.K. Zhang, P.Y. Li, C. Yuan, Preparation and characterization of an ion exchanger based on semi-carbonized polyacrylonitrile fiber, *React. Funct. Polym.*, 68 (2008) 891–898.
- [29] B. Li, L. Yang, C.Q. Wang, Q.P. Zhang, Q.C. Liu, Y.D. Li, R. Xiao, Adsorption of Cd(II) from aqueous solutions by rape straw biochar derived from different modification processes, *Chemosphere*, 175 (2017) 332–340.
- [30] S.V. Manjunath, R.S. Baghel, M. Kumar, Antagonistic and synergistic analysis of antibiotic adsorption on *Prosopis juliflora* activated carbon in multicomponent systems, *Chem. Eng. J.*, 381 (2020) 122713, doi: 10.1016/j.cej.2019.122713.
- [31] Z.F. Liu, W.B. Li, Q. Liang, X. Fang, H.Y. Deng, Environmental effects on antibiotic adsorption by Fe/Mn-loaded amphoteric clay, *Desal. Water Treat.*, 265 (2022) 146–156.
- [32] D.S. Wang, Y. Chao, T. Zhang, Adsorption character of oxytetracycline and effect of pH on adsorption of oxytetracycline in soil, *Adv. Mater. Res.*, 864/867 (2013) 179–183.
- [33] R.A. Figueroa, A. Leonard, A.A. Mackay, Modeling tetracycline antibiotic sorption to clays, *Environ. Sci. Technol.*, 38 (2004) 476–483.